C-13 MAS NMR evidence for structural similarity of L162YL mutant and Rhodobacter sphaeroides R26 RC, despite widely different cytochrome c(2)-mediated re-reduction kinetics of the oxidized primary donor

Rossum, B.J. van; Wachtveitl, J.; Raap, J.; Hoef, K. van der; Gast, P.; Lugtenburg, J.; ... ; Groot, H.J.M. de

ELSEVIER

Spectrochimica Acta Part A 53 (1997) 2201–2208

SPECTROCHIMICA ACTA PART A

^{13}C MAS NMR evidence for structural similarity of L162YL mutant and *Rhodobacter sphaeroides* R26 RC, despite widely different cytochrome c_2-mediated re-reduction kinetics of the oxidized primary donor

B.-J. van Rossum [a], J. Wachtveitl [1,b], J. Raap [a], K. van der Hoef [a], P. Gast [c], J. Lugtenburg [a], D. Oesterhelt [b], H.J.M. de Groot [a,*]

[a] *Leiden Institute of Chemistry, Gorlaeus Laboratories, Leiden University, PO Box 9502, 2300 RA Leiden, The Netherlands*
[b] *Department of Membrane Biochemistry, Max-Planck Institute for Biochemistry, 82152 Martinsried, München, Germany*
[c] *Biophysics Department, Huygens Laboratory, Leiden University, PO Box 9502, 2300 RA Leiden, The Netherlands*

Received 23 December 1996; received in revised form 23 April 1997; accepted 23 April 1997

Abstract

CP/MAS NMR data collected from L162YL mutant [4′-^{13}C]Tyr-enriched *Rhodobacter sphaeroides* RCs reveal that Tyr L162 is in a slightly heterogeneous and probably rigid section of the protein complex. The differences in chemical shifts of the individual components relative to those of the [4′-^{13}C]Tyr *Rhodobacter sphaeroides* R26 response are 0.2 ppm or less. This is small compared to the total dispersion of [4′-^{13}C] isotropic shifts, ~5 ppm, which measures the shift range due to variations in the microscopic environment between the various tyrosines in the protein complex. The structural changes in the mutant with respect to *Rhodobacter sphaeroides* R26, as probed by the labels, are thus minimal on the scale of the NMR. This suggests that the dramatic decrease of re-reduction rate of the oxidized primary donor P upon mutation (Farchaus et al., Biochemistry 32 (1993) 10885–10893) cannot be attributed to significant structural changes in the protein. Hence the NMR is in line with the current view that the decrease of the re-reduction rate in the mutant originates from slow reorientation of the docked cytochrome. © 1997 Elsevier Science B.V.

Keywords: Photosynthesis; Isotope labeling; MAS NMR; R26; Mutant

1. Introduction

The primary processes of photosynthesis in the photosynthetic bacterium *Rhodobacter* (*Rb.*) *sphaeroides* comprise a light-induced charge separation by which excitation energy is converted into chemical energy. This charge separation occurs in the photosynthetic reaction center (RC), a

* Corresponding author. Tel.: +31 71 5274539; fax: 31 71 5274537; e-mail: degroot@rulg18.leidenuniv.nl.

[1] Present address: Institut für Medizinische Optik, Ludwig-Maximilians-Universität, Barbarastr. 16, 80797 München, Germany.

PII S1386-1425(97)00114-5

transmembrane protein complex consisting of three polypeptide chains, the L, M and H subunits. Two bacteriochlorophyll (BChl) *a* molecules at the periplasmic side form a dimer, the special pair (P) [1–3]. Upon illumination, P is photooxidized and an electron is transferred to the cytoplasmic side along the cofactors on the A branch. The charge separation is stabilized by the re-reduction of P^+ by a soluble cytochrome (cyt) c_2.

It has been shown [4] that the residue Tyr L162, which is conserved between different RCs [5–7], and which is located close to P at the periplasmic side, plays an important role in the kinetics of P^+ re-reduction. It was suggested that cyt c_2 is bound or docked to the LM complex at the periplasmic side of the membrane [8], with the aromatic ring of Tyr L162 located almost midway between the tetrapyrrole rings of P and the heme ring of cyt c_2. However, according to a recent characterization of the RC-cyt c_2 co-crystal structure, the cytochrome is located at the periplasmic side adjacent to the M subunit, which increases the distance between the heme and P to about 14 Å [9], and for this reason it is difficult to imagine that an electron-transfer pathway involves Tyr L162 [9], although it was calculated that this residue is most strongly coupled to the dimer P [10]. For intact cells of *Rb. sphaeroides*, the in vivo kinetics of the P^+ re-reduction can be described in terms of three distinct phases [11]. Substitution of another amino acid for Tyr L162 in *Rb. sphaeroides* resulted in a loss or a drastic reduction of the fastest component of the in vivo P^+ re-reduction rate, which for the native RCs has a half-time of ~ 5 μs and a contribution of 46% [4,12]. This can be contrasted with the kinetics of the P^+ re-reduction found for RCs from *Rhodopseudomonas* (*Rps.*) *viridis* with the cytochrome tightly bound to the LM complex [13]. In that case four kinetic components are required to fit the re-reduction kinetics of P^+ by the nearest heme of the cytochrome, but only the fastest phase with a characteristic time of 0.19 μs is dominant, since it comprises 76% of the total change involved in the re-reduction [14,15]. It was suggested that the absence of the fast phase observed in the *Rb. sphaeroides* mutants was due to a domination of states with cyt c_2 non-productively bound to the RC, and to a reduction upon mutation in the reorientation rate from a non-productively to a productively bound cyt c_2, rather than to the effect of L162 on the electron-transfer rate alone [12]. Taking into account the relatively long distance between the special pair and cyt c_2, as well as the logarithmic relationship between electron-transfer rate and distance reported for the various charge transfer events in RCs [16], it is indeed unlikely that substitution of Tyr L162 would provoke the loss of the fast phase purely by an effect on the re-reduction rate, unless the substitution is associated in some way by considerable structural changes in the protein complex.

In this work ^{13}C cross-polarization magic angle spinning (CP/MAS) nuclear magnetic resonance (NMR) data from mutant RCs L162YL, i.e. with leucine substituted for tyrosine L162 and enriched with [4′-^{13}C]Tyr, are presented. MAS NMR in combination with site-specific isotope enrichment is at present the only technique that provides clear access to such important characteristics of the protein as the local spatial and electronic structure around amino acid side chains, and local dynamic properties. To address structural effects of the L162YL substitution on the protein, the spectra from the mutant are compared with NMR data collected from [4′-^{13}C]Tyr-enriched RCs from *Rb. sphaeroides* R26 [17,18] and the [4′-^{13}C]Tyr-enriched mutant M210YW [19], a protein modification which involves a tyrosine located at the acceptor side of the special pair.

2. Experimental

Site-directed mutants of *Rb. sphaeroides* were engineered to substitute Leu for Tyr L162. The mutation was expressed in the *Rb. sphaeroides puf* deletion strain pufΔLMX21/3, a neurosporene accumulator, as described in detail elsewhere [4,20]. Highly enriched (99%) [4′-^{13}C]Tyr (Fig. 1, inset) was synthesized as described in Refs. [19,21], and cells of mutant *Rb. sphaeroides* were grown in a synthetic medium containing the highly enriched [4′-^{13}C]Tyr [22]. RCs were isolated using a slightly modified version of the methods described in Ref.

[23]. Chromatophores ($OD^{865} = 33$) were incubated three times (1×45 min; 2×30 min) with 0.25% LDAO (*N,N*-dimethyldodecylamine-*N*-oxide) in 0.1 M potassium phosphate (pH 7.5) at room temperature. After centrifugation at $300\,000 \times g$ for 120 min, the supernatant from the first incubation contained mainly light-harvesting complexes (LHC I and II) and was discarded, while the supernatant from the second and third incubations contained the RCs with variable LHC-contamination. Next the RCs were precipitated with ammonium sulphate (30% w/v), and the floating pellet was resuspended in 0.1% LDAO, 10 mM Tris and 1 mM EDTA (pH 8), followed by desalting on a Sephadex G-50 column. Subsequently the RCs were loaded on a Poros-50 MQ (Perseptive Biosystems, Cambridge MA, USA) column. After washing the RCs briefly with 0.1% LDAO, 10 mM Tris and 1 mM EDTA (pH 8), a salt gradient (0–300 mM NaCl) was applied. The RCs eluted from the column at about 200 mM NaCl. With this procedure any residual LHC-contamination remained on the column. A typical A_{280}/A_{800} ratio of 1.4 was measured for the RC preparation. Finally the RCs were concentrated to an OD^{800} of 330, corresponding to about 1 mM RC, using a Filtron 100-kDa filter. The NMR data presented in this paper were collected from 300 µl of the detergent-solubilized RCs. Before and after taking the CP/MAS NMR data on the RCs, electronic absorption spectra were measured (vide infra), and no change in the absorption spectrum was found, which confirms that the integrity and quality of the sample were maintained during the NMR measurement procedure.

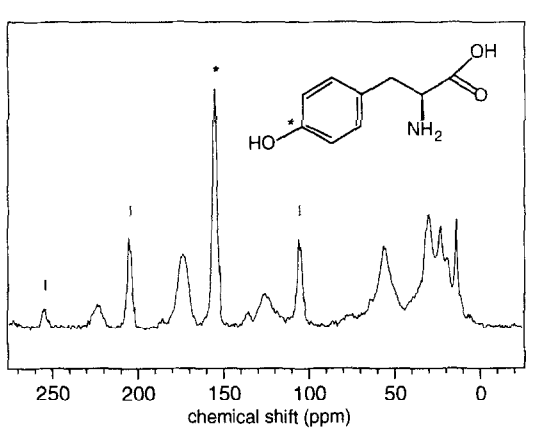

Fig. 1. CP/MAS spectroscopy of [4'-^{13}C]Tyr L162YL at T = 230 K with $\omega_r/2\pi = 5$ kHz. (*) indicates the centerband signals and (|) the sideband signals from the labels. The inset shows the structure of L-Tyr. The carbon labeling is indicated with an asterisk.

The 100-MHz ^{13}C CP/MAS NMR spectra were obtained using a MSL-400 NMR spectrometer with a 7-mm MAS probe (Bruker, Karlsruhe, Germany). Before starting NMR experiments at moderately high spinning speeds, $\omega_r/2\pi = 5$ kHz, the sample was frozen with liquid nitrogen-cooled bearing gas [18] with the rotor spinning with a low speed of $\omega_r/2\pi \approx 1$ kHz to ensure a homogeneous sample distribution against the rotor-wall. The bearing gas temperature T_B was measured just before the gas entered the spinning assembly and the temperature of the sample can be approximated by $T \approx 0.86 \cdot T_B +$ 50 K($\pm$ 5 K). A home-built spinning speed controller was used to keep the spinning rate constant [24]. The spectra were recorded with 3500 datapoints and zero filled to 8192 points. During acquisition the protons were decoupled with continuous wave irradiation. The ^{1}H 90° pulse length was determined to be 4.2 µs. Data were collected with a mixing time of 1 ms, a recycle delay of 3.0 s, a 10-µs dead time delay and a sweep-width of 50 kHz. All spectra are relative to tetramethylsilane (TMS), using the prominent LDAO signal at 14.4 ppm for internal calibration. The actual data presented here were collected in two subsequent sets which were added after Fourier transformation. The first-order phase corrections after Fourier transformation were kept almost equal for the two data sets, -67 and $-71°$. The absolute error in the chemical shift is estimated to be ~ 0.2 ppm [18].

Spectral deconvolutions and semi-empirical calculations were performed with an Indy workstation (Silicon Graphics, Mountain View, CA, USA)

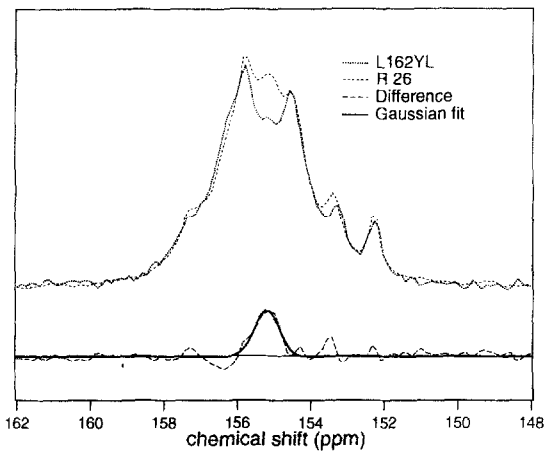

Fig. 2. CP/MAS difference spectroscopy of [4′-^{13}C]Tyr *Rb. sphaeroides* R26 minus [4′-^{13}C]Tyr L162YL at $T = 230$ K. The thick solid line represents the least-squares fit of the difference spectrum with a Gaussian line.

3. Results

The use of high-resolution solid-state NMR in conjunction with selective isotope enrichment and site-directed mutagenesis is a powerful technique to characterize photosynthetic components and other large membrane protein complexes with atomic selectivity [25]. In particular, this approach provides access to microscopic information regarding possible structural and electrostatic heterogeneities and the dynamic properties of the protein interior.

Low-temperature magic angle spinning NMR was used to study *Rb. sphaeroides* L162YL mutant RCs enriched with [4′-^{13}C]Tyr at $T = 230$ K (Fig. 1). The strong signals around 205, 155 and 105 ppm are associated with the isotope labels. The centerband responses are the signals around 155 ppm, indicated with an asterisk. The chemical shifts of the natural abundance ^{13}C background signals of the aliphatic carbons are between 0 and 75 ppm, while the natural abundance ^{13}C of the peptide carbonyls resonates at ~ 175 ppm. The NMR response from the labels comprises various narrow lines superimposed on a broad doublet.

To resolve the contribution of the [4′-^{13}C] of Tyr L162 to the spectrum of R26 RC [18], a comparison between the data for the mutant and the R26 was made. Difference spectroscopy (Fig. 2) of the signal of the [4′-^{13}C] Tyr *Rb. sphaeroides* R26 (data taken from Ref. [19]) minus the signal of the [4′-^{13}C]Tyr L162YL mutant measured at $T \sim 230$ K with $\omega_r/2\pi = 5$ kHz and scaled to minimize the intensity of the difference, reveals a Gaussian-type contribution that is attributed to Tyr L162. A least-squares fit of the difference spectrum performed with a single Gaussian with a chemical shift of 155.2 ± 0.1 ppm yields an estimate of the linewidth of 80 Hz. The intensity corresponds to $\sim 5\%$ of the total [4′-^{13}C]Tyr signal. The residuals around 153.5 and 157 ppm are of dispersive character and may reflect minor changes of the chemical environment of tyrosines that have not yet been assigned. They may be associated with the mutation, but it cannot be excluded at this point that other minor differences between the two species, for instance the presence of the carotenoid neurosporene in the mutant RCs, can give rise to small local changes of the spatial or electronic structure, affecting a tyrosine side-chain NMR response. Apart from the suppression of the intensity around 155.2 ppm by the mutation, this is the largest difference between the NMR spectra of the two samples.

To address the possibility of global structural changes in the protein associated with the mutation, we follow the same procedure as used previously by Shochat et al. [19]. This requires a phenomenological decomposition of the signal from the mutant after subtraction of the natural abundance response. In Figs. 3 and 4 the difference signals, i.e. the signals of the [4′-^{13}C]Tyr minus the natural abundance background, and their second derivatives, were deconvoluted with a superposition of Lorentzian lines using previously established procedures [18,19]. The deconvolution reported by Fischer et al. [18] for the [4′-^{13}C]Tyr-enriched *Rb. sphaeroides* R26 RCs served as an initial guess for the deconvolution reported in this work. Interestingly, this basic 'fingerprint' pattern obtained by Fischer et al. [18] requires only minor adjustments to represent the L162YL data. The results after least-squares minimisation are summarized in Table 1, and are compared with the results reported by Fischer et al. [18]. As in the earlier studies, most of the [4′-^{13}C]Tyr NMR re-

sponse of the RC (Fig. 3) is divided over two broader components. The second derivative signal in Fig. 4a clearly shows the characteristic [4′-^{13}C]Tyr second derivative fingerprint pattern of four pronounced minima near 155.7, 154.5, 153.2 and 152.2 ppm and three less-pronounced minima near 157.3, 156.3 and 155.0 ppm (Table 1). From the comparison with the signal of enriched *Rb. sphaeroides* R26 in Fig. 4b, it is evident that the second derivative signals from the mutant and the [4′-^{13}C]Tyr in *Rb. sphaeroides* R26 are highly similar. Thus, the L162 label response is not resolved in the second derivative spectrum of the R26. There is only a difference in the intensity of the second derivative response around 155 ppm between Figs. 4A and 4B. The L162 label response is also not resolved in Fig. 3B. The chemical shifts and linewidths in the deconvolution analysis of the L162YL mutant closely resemble the sets found for the [4′-^{13}C]Tyr-enriched *Rb. sphaeroides* R26 and also compares extremely well with the second derivative signal of the [4′-^{13}C]Tyr-enriched mutant M210YW (see Ref. [19]). The differences in chemical shifts of the individual components relative to those of the [4′-^{13}C]Tyr *Rb. sphaeroides* R26 response are 0.2 ppm or less (cf. Table 1). This is small, considering the total dispersion of 4′-^{13}C isotropic shifts, ~5 ppm, which measures the variations in the microscopic environment between the various tyrosines in the protein complex (cf. Figs. 2 and 3). In aromatic and conjugated systems a charge density variation of one positive electronic equivalent translates into a positive carbon shift of about 155–160 ppm [26,27]. It is thus concluded that the shift differences indicate only small local charge variations of $\leq 2 \times 10^{-3}$ electronic equivalents, reflecting little difference in electronic structure between the two species on the scale of the NMR.

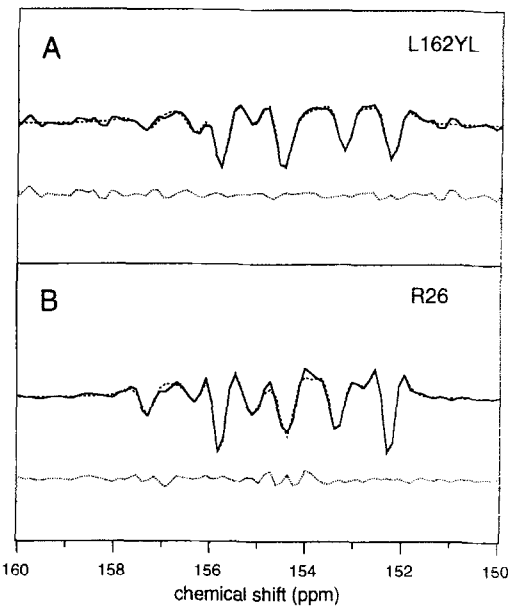

Fig. 4. Second derivatives of the data (solid lines), the fits (dashed lines), and the residuals (data minus fit, dotted lines) of the signal from L162YL (A) and *Rb. sphaeroides* R26 (B, data taken from Ref. [18]).

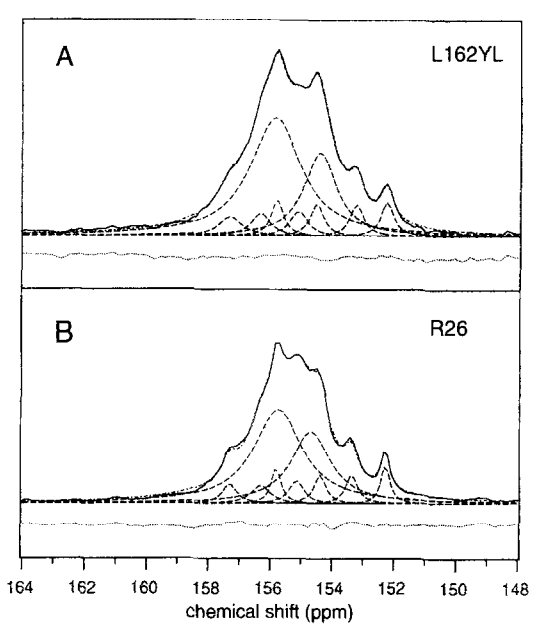

Fig. 3. Comparison of L162YL (A) with *Rb. sphaeroides* R26 (B, data taken from Ref. [18]). Data are represented by solid lines, fits by dot-dashed lines and individual contributions to each fit are dashed. The residuals (data minus fit) are shown as dotted lines.

Finally, the absorption spectrum of the RCs of the mutant L162YL obtained before the NMR experiment is shown in Fig. 5, together with the absorption spectrum of *Rb. sphaeroides* R26. The A_{280}/A_{800} ratios measured before and after the NMR experiment were 1.34 and 1.36, respec-

Table 1
Deconvolution of the [4′-^{13}C]Tyr response (centerband) of the CP/MAS spectra of the mutant RCs L162YL and of the *Rb. sphaeroides* R26 RCs[a]

L162YL		Wild type [18,19]		
σ_i (ppm)	FWHM (Hz)	σ_i (ppm)	FWHM (Hz)	Component
155.8	186	155.7	192	a
154.4	114	154.6	154	b
157.3	76	157.2	57	i
156.3	64	156.2	75	ii
155.7	36	155.7	37	iii
155.0	57	155.1	58	iv
154.5	40	154.3	46	v
153.2	42	153.3	46	vi
152.2	37	152.2	34	M210[b]

Isotropic chemical shifts (σ_i, in ppm relative to TMS) and linewidths (FWHM) of the two broad components (a,b) and the small narrow lines (i–vii) are listed. Prior to Fourier transforming the data and deconvoluting the spectra, a 12-Hz exponential apodization was applied.
[a]data from Ref [18].
[b]M210 was previously assigned using a M210YW mutant [19].

tively, which confirms that a good sample quality was maintained during the NMR experiment.

4. Discussion

From the NMR difference spectroscopy (Fig. 2), the response of Tyr L162 in *Rb. sphaeroides* is assigned to a signal at 155.2 ppm, in between the two broader components of the [4′-^{13}C]Tyr NMR response of the mutant. Previously, the broad downfield component was tentatively associated with residues in polar sections of the complex, whereas the upfield component was attributed to residues in apolar environments [18]. In this respect, in the recent X-ray structure for *Rb. sphaeroides* from Ermler et al. [28], a water molecule is positioned within hydrogen bonding distance of the L162 phenolic oxygen, while the crystallographic data for the similar *Rps. viridis* RC complex indicate that the equivalent of Tyr L162 is also in contact with a water molecule, see Ref. [4] and references therein. Because of the assignment of Tyr L162 in *Rb. sphaeroides* R26 to a signal in between the two broad components, it is consistent with the X-ray data and the previous NMR interpretations.

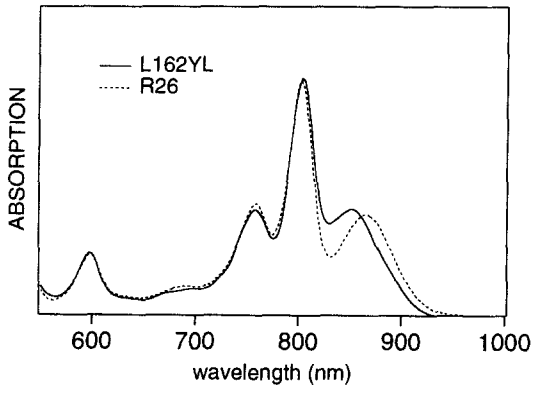

Fig. 5. Absorption spectrum from isolated RCs of the mutant L162YL (solid line) and of *Rb. sphaeroides* R26 (dashed line).

In contrast to the response of Tyr M210 on the other side of the special pair at 152.2 ppm, which provided strong evidence that Tyr M210 is in a structurally and functionally homogeneous region of the RC protein complex [19], the linewidth of 80 Hz reveals that Tyr L162 in *Rb. sphaeroides* R26 is in a slightly heterogeneous but probably still rigid region of the RC protein complex. The similarity of the sets of lines (cf. Table 1) used to deconvolute the [4′-^{13}C]Tyr response of the *Rb. sphaeroides* R26 RCs [17,18] and of the L162YL mutant RCs, provides strong evidence against pronounced structural changes upon mutation. For instance, for *Rb. sphaeroides* R26 some very small signal remains around the minimum near 154.5 ppm after deconvolution of the second derivatives, which appears to be somewhat systematic, since it was also observed for the M210YW mutant. The absence of this spectral feature for L162YL may indicate a change in the mutant, but such effects are very small on the scale of the NMR. Hence the most rigid and well-defined parts of the protein, most notably the *trans*-membrane region of the complex, are essentially not affected by the mutation. The absorption spectrum globally supports this picture (cf. Fig. 5). In particular, the unique environment of Tyr M210 is hardly affected upon substitution, as is reflected by an almost identical NMR response

in the mutant, with respect to isotropic shifts and line widths from the ^{13}C labels.

In Fig. 5, the Q_Y transition of the special pair in the mutant is down-shifted from the value of 866 nm in the chromatophore to 852 nm in the RC, corresponding to a change in energy of about 0.02 eV. Several authors have reported a detergent-dependent shift of the P-band already for wild-type RCs, see e.g. Ref. [4]. In the mutant this shift is observed for relatively low detergent concentrations [4], and was tentatively attributed to increased instability with respect to structural perturbations associated with the amount of detergent [4]. However, another possibility may be that, e.g., water molecules fill the space left by the tyrosine in the mutant, giving rise to a more polar environment of the special pair. In addition Parson et al. [29] have argued that electrostatic interactions with tyrosine side chains may already be of importance for the P electronic properties. In order to check for possible electrostatic effects associated with the mutation, we performed semi-empirical calculations using the MOPAC package. Starting with the atomic coordinates from the X-ray data for *Rb. sphaeroides* from Ermler et al. [28] for the bacteriochlorophyll dimer, the two adjacent histidines L173 and M200 coordinating the Mg^{2+} ion, and the tyrosine L162, the dimer structure was minimized using the standard PM3 parametrization included with the package, while fixing the coordinates of the L162 phenolic oxygen, of both magnesium atoms and of their coordinating nitrogen atoms. In this way a set of approximate electronic eigenvalues were obtained, in agreement with recently reported values calculated by Scherer et al. [30]. To estimate the direct electrostatic effect of the tyrosine on the electronic structure of the special pair, and to simulate the mutation, we separated the tyrosine from the special pair in the virtual reality of the computer by shifting it 30 Å from the dimer. Subsequently, only the electronic structure was recalculated, without further minimization. It was found that shifts of ~ 0.02 eV of individual electronic energy levels can occur upon displacement of the tyrosine side chain. Our calculations indicate that the observed down-shift of the Q_Y could in principle arise from electrostatic effects, which, for isolated RCs, might be influenced by the detergent concentration [4].

The three different phases of the kinetics of the P^+ re-reduction were attributed to productively bound, non-productively bound/docked and unbound cytochromes [11,12]. The suppression of the fastest phase upon substitution for Tyr L162 in RCs from *Rb. sphaeroides* was previously attributed to a decrease of the reorientation rate from a non-productively to a productively bound cyt c_2, rather than to a reduction of the electron-transfer rate [12]. In line with this hypothesis, it was found that Tyr L162 in *Rps. viridis* RCs with strongly bound cytochrome can be substituted by several residues without affecting the fastest component of the kinetics of the P^+ re-reduction by more than one order of magnitude [31].

The association, dissociation and reorientation phenomena for the *Rb. sphaeroides* RC and its L162 mutants have been studied by Wachtveitl et al. [12]. It appears that the two steps of cyt binding/reorientation are of different nature. The binding is mainly due to global electrostatic properties of the two proteins involved, and leads to unproductively attached cyt c_2. This should not be very sensitive to the L162YL mutation [12]. In particular, there is no significant difference in the binding constant between the R26 and the L162YL mutant. However, a reorientation of the bound cyt c_2 is thought to lead to the productive state. This state, or the motion towards this state, is sensitive to L162 point mutations, as can be concluded from the suppression of the fast kinetic component in all L162 mutants studied thus far [12].

The results of the NMR measurements are consistent with the reorientation hypothesis, since no evidence for pronounced structural changes in the protein was found, while the long-distance electron transfer rate in the productive state is thought to depend mainly on the distance between donor and acceptor [16]. In this respect, several tyrosines are positioned near P at the periplasmic side, where the largest structural effects upon the mutation could be expected. In particular the highly similar second-derivative fingerprint-pattern in the NMR response of the [4′-^{13}C]Tyr of the mutant L162YL reveals that the environment

probed by the resolved tyrosines is virtually unaffected by the mutation. For instance, in order to affect the electron transfer from the heme to P by more than one order of magnitude, a significant repositioning of P in the protein would be anticipated. It is difficult to imagine such a structural change without affecting the signal of Tyr M210 which is located between the special pair, the bacteriochlorophyll and the bacteriopheophytin on the A branch. This inference is also confirmed by the absorption spectrum (Fig. 5) and other available spectroscopic data [4]. The structural similarity found for L162YL with respect to R26 supports previous inferences that the function of tyrosine L162 is not to intervene directly and to facilitate the electron-transfer between cyt c_2 and P^+, but rather to fine-tune a fragile cyt c_2–RC docking/reorientation processes. Alternatively, there could still be a direct mechanism of importance for the re-reduction involving specific interactions between the tyrosine and the donor, which is affected by the mutation.

Acknowledgements

We wish to thank S.J. Jansen for culturing the cells and isolating the reaction centers.

References

[1] J. Deisenhofer, H. Michel, EMBO J. 8 (1989) 2149.
[2] D.C. Rees, H. Komiya, T.O. Yeates, J.P. Allen, G. Feher, Ann. Rev. Biochem. 58 (1989) 607.
[3] C.H. Chang, O. El Kabbani, D. Tiede, J. Norris, M. Schiffer, Biochemistry 30 (1991) 5352.
[4] J.W. Farchaus, J. Wachtveitl, P. Mathis, D. Oesterhelt, Biochemistry 32 (1993) 10885.
[5] J.C. Williams, L.A. Steiner, R.C. Ogden, M.I. Simon, G. Feher, Proc. Natl. Acad. Sci. USA 80 (1983) 6505.
[6] D.C. Youvan, E.J. Bylina, M. Alberti, Cell 37 (1984) 949.
[7] J.A. Shiozawa, F. Lottspeich, D. Oesterhelt, R. Feick, Eur. J. Biochem. 180 (1989) 75.
[8] J.P. Allen, G. Feher, T.O. Yeates, H. Komiya, D.C. Rees, Proc. Natl. Acad. Sci. USA 84 (1987) 6162.
[9] N. Adir, H.L. Axelrod, P. Beroza, R.A. Isaacson, S.H. Rongey, M.Y. Okamura, G. Feher, Biochemistry 35 (1996) 2535.
[10] A.J.A. Aquino, P. Beroza, D.N. Beratan, J.N. Onuchic, J. Chem. Phys. 197 (1995) 277.
[11] R.E. Overfield, C.A. Wraight, D. DeVault, FEBS Lett. 105 (1979) 137.
[12] J. Wachtveitl, J.W. Farchaus, P. Mathis, D. Oesterhelt, Biochemistry 32 (1993) 10894.
[13] J. Deisenhofer, O. Epp, K. Miki, R. Huber, H. Michel, Nature 318 (1985) 618.
[14] S.M. Dracheva, L.A. Drachev, A.A. Konstantinov, A.Y. Semenov, V.P. Skulachev, A.M. Arutjunjan, V.A. Shuvalov, S.M. Zaberezhnaya, Eur. J. Biochem. 171 (1988) 253.
[15] J.M. Ortega, P. Mathis, Biochemistry 32 (1993) 1141.
[16] C.C. Moser, J.M. Keske, K. Warncke, R.S. Farid, P.L. Dutton, Nature 355 (1992) 796.
[17] H.J.M. de Groot, J. Raap, C. Winkel, A.J. Hoff, J. Lugtenburg, Chem. Phys. Lett. 169 (1990) 307.
[18] M.R. Fischer, H.J.M. de Groot, J. Raap, C. Winkel, A.J. Hoff, J. Lugtenburg, Biochemistry 31 (1992) 11038.
[19] S. Shochat, P. Gast, A.J. Hoff, G.J. Boender, S. van Leeuwen, W.B.S. van Liemt, E. Vijgenboom, J. Raap, J. Lugtenburg, H.J.M. de Groot, Spectrochim. Acta 51A (1995) 135.
[20] J.W. Farchaus, D. Oesterhelt, EMBO J. 8 (1989) 47.
[21] C. Winkel, M.W.M.M. Aarts, F.R. van der Heide, E.G. Buitenhuis, J. Lugtenburg, Recl. Trav. Chim. Pays-Bas 108 (1989) 139.
[22] J. Raap, C. Winkel, A.H.M. de Wit, A.H.H. van Houten, A.J. Hoff, J. Lugtenburg, Anal. Biochem. 191 (1990) 9.
[23] S. Shochat, T. Arlt, C. Francke, P. Gast, P.I. van Noort, S.C.M. Otte, H.P.M. Schelvis, S. Schmidt, E. Vijgenboom, J. Vrieze, W. Zinth, A.J. Hoff, Photosyn. Res. 40 (1994) 55.
[24] H.J.M. de Groot, V. Copie, S.O. Smith, P.J. Allen, C. Winkel, J. Lugtenburg, J. Herzfeld, R.G. Griffin, J. Magn. Res. 77 (1988) 251.
[25] H.J.M. de Groot, in: J. Amesz, A.J. Hoff (Eds.), Biophysical Techniques in Photosynthesis, Advances in Photosynthesis, vol. 3, Kluwer Academic Publishers, Dordrecht, 1996, pp. 299–313.
[26] H. Spiesecke, W.G. Schneider, Tetrahedron Lett. 14 (1961) 468.
[27] H. Strub, A.J. Beeler, D.M. Grant, J. Michl, P.W. Cutts, K. Zilm, J. Am. Chem. Soc. 105 (1983) 3333.
[28] U. Ermler, G. Fritzsch, S.K. Buchanan, H. Michel, Structure 2 (1994) 925.
[29] W.W. Parson, Z.-T. Chu, A. Warshel, Biochim. Biophys. Acta 1017 (1990) 251.
[30] P.O.J. Scherer, C. Scharnagl, F.S. Fischer, Chem. Phys. 197 (1995) 333.
[31] B. Dohse, P. Mathis, J. Wachtveitl, E. Laussermair, S. Iwata, H. Michel, D. Oesterhelt, Biochemistry 34 (1995) 11335.